Available online at www.sciencedirect.com
ScienceDirect
Scripta Materialia 65 (2011) 41–44
Scripta MATERIALIA
www.elsevier.com/locate/scriptamat

Effects of the antiferromagnetic anti-phase domain boundary on the magnetization processes in $Ni_2Mn(Ga_{0.5}Al_{0.5})$ Heusler alloy

R.Y. Umetsu,[a,*] H. Ishikawa,[b] K. Kobayashi,[b,1] A. Fujita,[b] K. Ishida[b] and R. Kainuma[b]

[a] *Institute for Materials Research, Tohoku University, Katahira 2-1-1, Sendai 980-8577, Japan*
[b] *Department of Materials Science, Graduate School of Engineering, Tohoku University, Sendai 980-8579, Japan*

Received 22 February 2011; revised 9 March 2011; accepted 10 March 2011
Available online 16 March 2011

The effects of anti-phase domain (APD) boundaries on the magnetic properties of $Ni_2Mn(Ga_{0.5}Al_{0.5})$ alloy were studied by magnetic measurements and transmission electron microscopic observations. The growth of APDs at 773 K followed the square root law for annealing time. While the saturation magnetization and the Curie temperature were hardly affected by the APD size, the magnetization curve in the specimen with smaller mean APD size became harder, caused by the pinning effect of the magnetic domain walls due to the APD boundaries.

Keywords: $Ni_2Mn(Ga,Al)$; Annealing time; Anti-phase domain boundary; Pinning of the magnetic domain wall; Magnetization process

Ferromagnetic shape memory alloys (FSMAs) have attracted considerable interest as a new type of materials applicable in actuators and sensors which can be controlled by external magnetic fields. Among the various FSMAs, the largest magnetic field-induced strain (MFIS), i.e. up to about 10%, has been reported in off-stoichiometric Ni_2MnGa single crystals [1]. The magnetic shape memory effect is caused by the magnetic-field-induced rearrangement of the twin variants, whose driving force is high magnetocrystalline anisotropy energy [2]. Besides the MFIS phenomenon, recent studies have also revealed that Ni_2MnGa alloys exhibit other attractive properties, such as large magnetoresistance and magnetocaloric effect [3–5]. It has also been found that the ferromagnetic parent phase with an $L2_1$-type structure in Ni–Mn–Al alloys transforms to the martensite phase with a long period stacking structure [6–9]. Additionally, a polycrystalline specimen of $Ni_{53}Mn_{25}Al_{22}$ alloy was found to exhibit MFIS behavior with a maximum value of about −100 ppm just above the martensitic transformation finishing temperature [9]. Although the magnetic moment and the Curie temperature (T_C) of the $L2_1$ phase in Ni_2MnAl alloy have been reported to be comparable to those in the Ni_2MnGa alloy according to theoretical calculations [10–12], the magnetic properties of Ni_2MnAl alloy are not in accord with the theoretical results, in contrast to Ni_2MnGa alloy [13]. Recently, our group investigated the phase stabilities, crystal structures and magnetic properties of $Ni_2Mn(Ga_xAl_{1-x})$ ($0 \leqslant x \leqslant 1$) alloys to determine the origin of the difference in the magnetic properties between Ni_2MnAl and Ni_2MnGa, and also to clarify effects of the degree of $L2_1$ long-range order on magnetic properties in $Ni_2Mn(Ga_{0.5}Al_{0.5})$ alloy [14]. The magnetization and the T_C of $Ni_2Mn(Ga_{0.5}Al_{0.5})$ alloy are functions of the annealing temperature, which suggests that these magnetic properties are affected by the degree of long-range order for the specimen. It was also confirmed by electron holography and Lorentz microscopy that most of the magnetic domain walls (MDWs) in $Ni_2Mn(Ga_{0.5}Al_{0.5})$ alloy with the $L2_1$ structure are superimposed with the anti-phase domain (APD) boundaries that act as pinning sites for migration of the MDWs in the magnetization process [15]. In the present study, we investigated the influences of the APD size on the magnetic properties by using some $Ni_2Mn(Ga_{0.5}Al_{0.5})$ specimens with different mean APD sizes.

$Ni_2Mn(Ga_{0.5}Al_{0.5})$ alloy was prepared from high-purity Ni (99.9%), Mn (99.7%), Ga (99.99%) and Al (99.7%) by induction furnace melting under an argon gas atmosphere. Small specimens cut from the ingots were sealed in quartz tubes after being wrapped in molybdenum foil to prevent reaction with the quartz tubes. They were annealed at 1273 K for 3 days as a solution heat treatment and subsequently quenched into

* Corresponding author. E-mail: rieume@imr.tohoku.ac.jp
[1] Present address: Technical Division, Department of Instrumental Analysis, School of Engineering, Tohoku University, Aoba 6-6-11, Sendai 980-8579, Japan.

1359-6462/$ - see front matter © 2011 Acta Materialia Inc. Published by Elsevier Ltd. All rights reserved.
doi:10.1016/j.scriptamat.2011.03.014

ice water, and additionally annealed at 773 K for 0.25, 4 and 24 h. Magnetic measurements with a superconducting quantum interference device magnetometer were carried out with using the small granular polycrystalline specimens of 1–3 mg weight. Microstructural observations were performed by transmission electron microscopy (TEM).

Figure 1 shows the thermomagnetization curves obtained under a magnetic field of 500 Oe for the specimens annealed at 773 K for 0.25, 4 and 24 h. The Curie temperatures of these three specimens perfectly coincide with one another, although the magnetic anisotropy seems to be different. We have recently reported that the saturation magnetization (M_s) and the T_C for the $Ni_2Mn(Ga_xAl_{1-x})$ alloys are significantly sensitive to the degree of long-range order, which can be controlled by the annealing temperature, and that especially the T_C is a function of the final annealing temperature [14]. In all the present specimens where the annealing temperature was fixed at 773 K, the degree of long-range order can be equivalent, which must result in the coincidence of T_C.

The TEM dark-field images using the $(1\,1\,1)_{L2_1}$ ordered reflection of the $Ni_2Mn(Ga_{0.5}Al_{0.5})$ alloy annealed at 773 K for 0.25, 4 and 24 h are shown in Figure 2(a)–(c), respectively. The micrograph used for Figure 2(c) was previously reported in Ref. [14]. From these figures, the mean APD size is confirmed to increase with increasing annealing time. In our previous paper, it was shown in $Ni_2Mn(Ga_{0.5}Al_{0.5})$ alloy that the higher the annealing temperature, the larger the mean APD size becomes, whereas the degree of long-range order of the $L2_1$ structure also changes at the same time [14]. By the thermomagnetization curves and the TEM observations of Figures 1 and 2, it was confirmed that specimens with different mean APD sizes and a comparable degree of long-range order can be obtained by controlling the annealing time at 773 K.

In order to quantitatively analyze the growth rate of the APDs, the mean diameter of the APDs is estimated using the point-counting method under the assumption that all the APDs are spherical in shape [16]. In the present procedure, the TEM dark-field images including the APD microstructure are assigned to a hypothetical grid with the length of a side being l, as illustrated in Figure 3(a). The mean diameter of the APDs, $\langle D\rangle$, is given by the relation

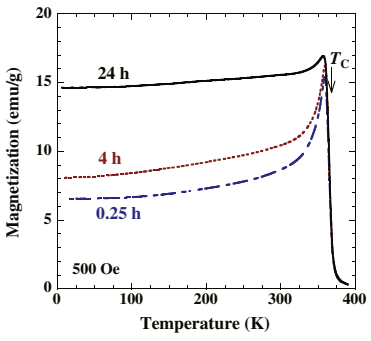

Figure 1. Thermomagnetization curves of $Ni_2Mn(Ga_{0.5}Al_{0.5})$ alloy annealed at 773 K for 0.25, 4 and 24 h measured under a magnetic field of 500 Oe. The arrow indicates the Curie temperature T_C.

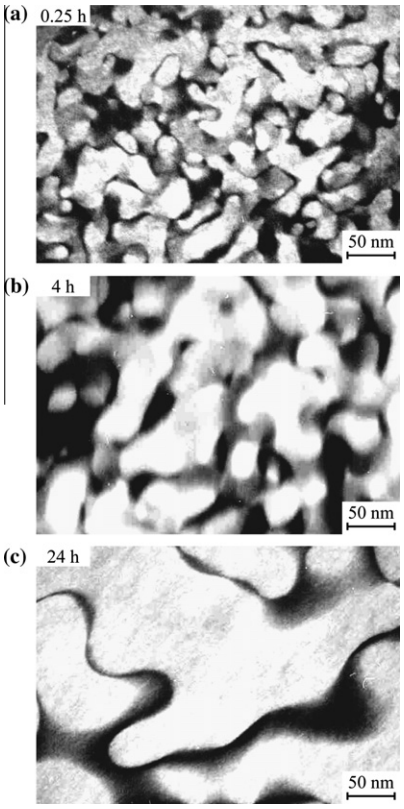

Figure 2. TEM dark-field images using the $(1\,1\,1)_{L2_1}$ ordered reflection taken from the $Ni_2Mn(Ga_{0.5}Al_{0.5})$ alloy annealed at 773 K for 0.25 (a), 4 (b) and 24 (c) h.

$$\langle D\rangle = \frac{lm}{N} \tag{1}$$

where m is the number of the side and N is the number of intersections between the grid and the APD boundaries. For example, in the case where l and m are set at 20 nm and 60, respectively, if the N is counted to be 40, as demonstrated in Figure 3(a), a value for $\langle D\rangle$ of 30 nm is obtained. By application of this method to the present TEM dark-field images, the $\langle D\rangle$ values for the specimens annealed at 773 K for 0.25, 4 and 24 h are evaluated as about 43, 78 and 168 nm, respectively. Figure 3(b) indicates the square of the mean APD size, $\langle D\rangle^2$, as a function of annealing time, t, at 773 K, where a linear relation between $\langle D\rangle^2$ and t is clearly shown. The kinetics of APD growth have been discussed by Allen and Cahn [17]. According to their microscopic diffusional theory for the motion of a curved APD boundary, the surface area in a unit volume of specimen, $S_v(t)$, at time t is given by

$$[S_v(t)]^{-2} - [S_v(0)]^{-2} = 2\phi M_b t \tag{2}$$

where $S_V(0)$ is the initial value of $S_v(t)$ and ϕ is the geometrical factor related to the shape of the APD structure. M_b is the boundary mobility, which has the same dimension as the diffusion coefficient ($m^2\,s^{-1}$) and is defined as $M_b = 2K\alpha$ [17], where K and α are the gradient energy coefficient and the kinetic coefficient in ordering, respectively. Since S_v is inversely proportional to $\langle D\rangle$, Eq. (2) can be modified as

$$\langle D(t)\rangle^2 - \langle D(0)\rangle^2 = k \cdot t \tag{3}$$